Climate change: vegetation and phenological phase dynamics

Yang Li

*College for Environment and Planning, Henan University, Kaifeng, Henan, China
and Key Laboratory of Geospatial Technology for Middle and Lower Yellow River
Region, Kaifeng, China*

Yaochen Qin

*College for Environment and Planning, Henan University, Kaifeng, Henan, China;
Key Laboratory of Geospatial Technology for Middle and Lower Yellow River
Region, Kaifeng, China and Collaborative Innovation Center of Urban-Rural
Coordinated Development, Zhengzhou, China, and*

Liqun Ma and Ziwu Pan

*College for Environment and Planning, Henan University, Kaifeng, Henan, China
and Key Laboratory of Geospatial Technology for Middle and Lower Yellow River
Region, Kaifeng, China*

Abstract

Purpose – The ecological environment of the Loess Plateau, China, is extremely fragile under the context of global warming. Over the past two decades, the vegetation of the Loess Plateau has undergone great changes. This paper aims to clarify the response mechanisms of vegetation to climate change, to provide support for the restoration and environmental treatment of vegetation on the Loess Plateau.

Design/methodology/approach – The Savitsky–Golay (S-G) filtering algorithm was used to reconstruct time series of moderate resolution imaging spectroradiometer (MODIS) 13A2 data. Combined with trend analysis and partial correlation analysis, the influence of climate change on the phenology and enhanced vegetation index (EVI) during the growing season was described.

Findings – The S-G filtering algorithm is suitable for EVI reconstruction of the Loess Plateau. The date of start of growing season was found to gradually later along the Southeast–Northwest direction, whereas the date of the end of the growing season showed the opposite pattern and the length of the growing season gradually shortened. Vegetation EVI values decreased gradually from Southeast to Northwest. Vegetation changed significantly and showed clear differentiation according to different topographic factors. Vegetation correlated positively with precipitation from April to July and with temperature from August to November.

Originality/value – This study provides technical support for ecological environmental assessment, restoration of regional vegetation coverage and environmental governance of the Loess Plateau over the past

two decades. It also provides theoretical support for the prediction model of vegetation phenology changes based on remote sensing data.

1. Introduction

The Fifth Assessment Report of the Intergovernmental Panel On Climate Change (IPCC) reported that almost all parts of the world are experiencing climate warming; moreover, since 1950, precipitation in Asia has decreased significantly (IPCC, 2014). Vegetation and phenology are important indicators of regional climatic characteristics, and climatic conditions restrict the geographical distribution of vegetation (Wang *et al.*, 2016a). Studies of vegetation coverage, phenology and their response to global climate change are of great significance toward an understanding of the impacts of climate change on vegetation, terrestrial ecosystems and human life (Richardson *et al.*, 2013). Literature review shows that achievements have been made toward understanding changes of vegetation phenology and the effects of climate change (Thompson and Koenig, 2018; Silveira *et al.*, 2019). In theory and at the method research level, Zhao *et al.* (2014) compared the performance of geographical weighted regression (GWR) and ordinary least squares (OLS) methods for exploring the spatial variation relationships between the normalized difference vegetation index (NDVI) and climate factors. Zhao *et al.* (2014) found that GWR represented significant improvements of model performance over OLS. Sousa *et al.* (2019) presented a method that uses empirical orthogonal function analysis of a single spectral index to capture phenological parameters from satellite imagery and to characterize the spatiotemporal dynamics of vegetation phenology. At the level of empirical research, Baniya *et al.* (2019) used the Sen's slope and Mann Kendall test statistics to investigate changes in vegetation at the national and provincial scales in Nepal from 2000 to 2017 and found a significant increase of the NDVI. Moreira *et al.* (2019) evaluated the dynamic of phenological metrics based on enhanced vegetation index (EVI) for the period from 2001 to 2014 through the TIMESAT program and reported that the phenological pattern of Brazil was controlled by variations of air temperature. Deka *et al.* (2019) adopted the threshold method to extract phenological parameters of vegetation and showed that the correlation of temperature and vegetation NDVI was stronger than that of precipitation in India. Adole *et al.* (2019) conducted a systematic analysis of the relationship between phenological and driver factors using satellite data and identified the photoperiod as the dominant factor of vegetation phenology. These studies effectively show that the phenological period of vegetation changed significantly at a globally scale (Deka *et al.*, 2019; Merrick *et al.*, 2019).

As the most important ecological safety zone and a core agricultural and animal husbandry area in China, the environment of the Loess Plateau is extremely fragile because of the adverse effects of the harshness of natural conditions and human activities. Research on the vegetation dynamics and phenological periods as well as their correlation with climate change in the Loess Plateau can provide theoretical references for the selection of optimal species and can provide technical support for the formulation and implementation of ecologically sustainable development measures. A number of authors have recognized the importance of vegetation and phenological changes of the Loess Plateau. Zhang and Ren (2015) used a dynamic threshold to identify phenological parameters in Shaanxi Province (which is part of the Loess Plateau) and concluded that the vegetation phenology varies significantly with latitude. Liu *et al.* (2013) found that the vegetation NDVI of the study area increased and the response of the vegetation to precipitation and potential

evapotranspiration showed a time lag in the Three-River Headwater Region when employing linear regression, Hurst index and partial correlation analysis. Zhang *et al.* (2013) conducted the time-lag partial correlation analysis to study the response of vegetation coverage to air temperature and precipitation conditions on the Loess Plateau and found that air temperature exerted a stronger influence than precipitation. Xia *et al.* (2018) analyzed the correlation of the asymmetric day and night increase of temperature and vegetation growth over the past 30 years and found that the partial correlation coefficient between the maximum temperature and NDVI was positive in wet and cold regions and negative in semi-arid and arid regions.

The literature shows that various studies focused on the extraction of phenological periods, the identification of the characteristics of temporal and spatial changes of vegetation and phenological periods (Xia *et al.*, 2015; He *et al.*, 2018) and the underlying causes of these changes (Zhou *et al.*, 2016; Zhang *et al.*, 2018). These studies are based on the analysis of temporal and spatial characteristics of vegetation and phenological period. Several achievements have been made. However, many controversies still exist about the relationship between vegetation and climate change and therefore, the research methods and influence factor analysis need to be further developed. Furthermore, because of factors such as the number of observed sample points, the coverage area and relevant species, traditional phenological observation is rarely applied to biological communities or at larger scales (Xu *et al.*, 2014). In recent years, aerospace and unmanned aerial vehicle remote sensing technology has rapidly developed (Li *et al.*, 2019), thus providing regional and even global remote sensing image data. With longer time series, broad coverage, high spatial resolution and easier access, this remote sensing data has been increasingly used in the study of vegetation and phenological evolution (Song *et al.*, 2015; Xin *et al.*, 2015). Consequently, this study used long time series satellite data to investigate the vegetation dynamics of the Loess Plateau.

This study used an S-G filtering algorithm, integrated into the time series satellite data analysis tool (TIMESAT), to reconstruct MODIS-EVI over the Loess Plateau, which effectively removed pixels containing outliers and noise. Based on the reconstructed EVI time series, phenological information for the vegetation of the Loess Plateau was extracted and the spatial distribution of EVI and the changing trend of phenology during the growing season were analyzed. Finally, partial correlation analysis was used to assess the multi-dimensional response of vegetation to climate change to provide a basis for the environmental evaluation and climate change prediction of the Loess Plateau.

2. Data and methods

2.1 Study area

The Loess Plateau region (i.e. the transition zone from a humid and semi-humid climate to an arid and semi-arid climate) is located at 100°52′E-114°33′E, 33°41′N-41°16′N (Figure 1). It includes the provinces Qinghai, Gansu, Ningxia, Inner Mongolia, Shaanxi, Shanxi and Henan and has a total area of about 624,000 km². Previous research showed that this region is particularly sensitive to global climate change. Since the 1960s, the average annual temperature on the Loess Plateau has increased by 1.91°C and the average annual rainfall has decreased by 29.11 mm (Wang *et al.*, 2012). The Loess Plateau is subject to a most severe soil and water loss and the environment is extremely sensitive to climate change (Yang *et al.*, 2018). Since the end of the 20th century, China has implemented a series of ecological restoration projects, such as water and soil conservation and the Three-North Shelterbelt project; consequently, the regional environment has been restored satisfactorily (Li *et al.*, 2012). Vegetation types of the Loess Plateau from southeast to northwest show degradation

Figure 1.
Geographical location
of the Loess Plateau
and distribution map
of meteorological
stations
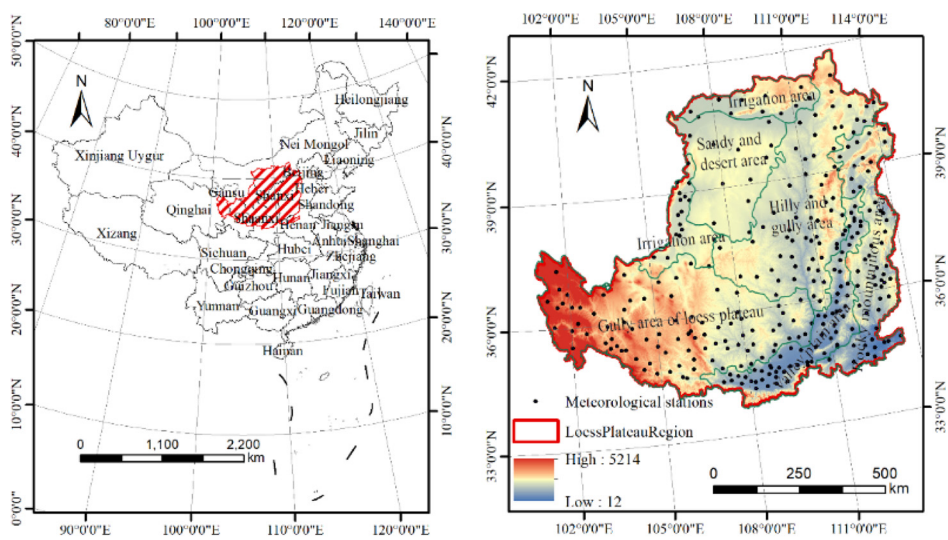
Source: Created by authors using ArcGIS (2019) solfware

from forest belt, forest grassland, typical grassland, desert grassland, to desert. The vegetation shows clear horizontal and vertical zonality because of factors such as temperature, precipitation and altitude.

2.2 Climate and terrain data set

The meteorological data for the Loess Plateau was obtained from the National Meteorological Information Center (http://data.cma.cn/). Digital elevation model (DEM) data was derived from the Geospatial Data Cloud (www.gscloud.cn) at a spatial resolution of 30 m. The DEM data as a covariable was adopted to the thin plate spline function to interpolate the monthly average temperature and precipitation data.

2.3 Enhanced vegetation index data set

The moderate resolution imaging spectroradiometer (MODIS) 13A2 EVI data sets from 2000 to 2018 were download from the National Aeronautics and Space Administration (https://search.earthdata.nasa.gov/). To study the vegetation change during the growing season and its correlation with climate factors, the EVI data set with a time resolution of 16 days was converted to a monthly scale by the maximum synthesis method. The average value of EVI in each month of the growing season was calculated as a representation of the state of vegetation coverage.

2.4 Time series data reconstruction and phenological data extraction

MODIS-EVI images were extracted, projected and transformed, mosaicked and clipped using a Python script. Because remote sensing image data is affected by aerosols, field of view, clouds and solar altitude angles (along with other conditions, such as outliers and noise), appropriate reconstruction of the time series data is a prerequisite for relevant research using MODIS-EVI. A time series data reconstruction method using

Fourier transform, known as the Savitsky–Golay (S-G) filter have been used by many authors (Madden, 1978; Jonsson and Eklundh, 2004). The advantage of this approach is that the degree of adaptation to the upper envelope can be tuned to the desired level, which differs from the maximum value composite method which always adapts the highest values (Stisen *et al.*, 2007). In addition, the vegetation index data set was reconstructed by the filtering algorithm, which retained the continuity of vegetation growth and its change, removed the influence of outliers and did not change the value of continuous change. Relevant studies have confirmed that this method produces a relatively ideal fit for the reconstruction of time series data (Borges *et al.*, 2014; Wang *et al.*, 2015; Duarte *et al.*, 2018). This study used the S-G filtering algorithm to reconstruct the EVI time series data to eliminate specific pixel values including mutation and noise. Because of the absence of MODIS-EVI time series data during the study period, images from the first three months of 2001 were supplemented to corresponding periods in 2000, based on relevant literature (Huang, 2009). The time series data before and after S-G fitting showed that the noise was significantly reduced (Figure 2).

2.5 Research methods
2.5.1 Savitsky–Golay filtering. S-G filtering is a moving window weighted average algorithm. Weighted coefficients are obtained using a least squares method fit for a given higher-order polynomial over a sliding window. The calculation formula for S-G filtering is shown in equation (1):

$$Y_j^* = \sum_{i=-m}^{i=m} \frac{C_i Y_{j+i}}{N} \tag{1}$$

where Y_j^* represents the reconstructed EVI value, y_{j+i} represents the original EVI value, C_i represents the coefficient obtained by S-G filtering, and N represents the number of convoluting integers, which is equal to the smoothing window size.

2.5.2 Trend analysis. Linear regression was used to calculate the temporal variability within vegetation parameters using raster data from the Loess Plateau based on an IDL script, and the F test was used for significance testing. The formula for calculating the slope is shown in equation (2):
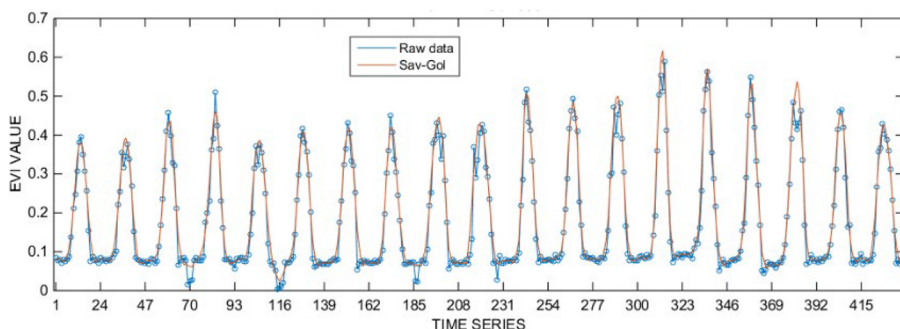

Source: Created by authors using TIMESAT (2019) solfware

$$\text{Slope} = \frac{n \times \sum\limits_{i=1}^{n} i \times P_i - \sum\limits_{i=1}^{n} i \sum\limits_{i=1}^{n} p_i}{n \times \sum\limits_{i=1}^{n} i^2 - \left(\sum\limits_{i=1}^{n} i \right)^2} \tag{2}$$

where Slope represents the change trend, P_i represents the phenology value for the ith year, and n represents the length of the time series. If the slope > 0, phenology is increasing; if the slope < 0, phenology is delayed; and if the slope = 0, phenology remains unchanged.

2.5.3 Partial correlation analysis. Partial correlation analysis can eliminate the interference of other variables and enable the study of the relationship between two target variables. In this study, the relationship between temperature and EVI over the vegetation growth season was analyzed by limiting precipitation variables. Then, the relationship between precipitation and vegetation EVI during growing season was analyzed by limiting temperature variables. First-order partial correlation coefficients were calculated based on the correlation coefficient formula (Cleophas and Zwinderman, 2018), as shown in equation (3):

$$r_{xy \cdot z} = \frac{r_{xy} - r_{xz} r_{yz}}{\sqrt{1 - r_{xz}^2} \sqrt{1 - r_{yz}^2}} \tag{3}$$

where, $r_{xy \cdot z}$ represents the partial correlation coefficient between x and y of the control variable z; r_{xz} represents the correlation coefficient between x and z; r_{yz} represents the correlation coefficient between y and z; and r_{xy} represents the correlation coefficient between x and y.

3. Results

3.1 Phenological spatial pattern and changes

3.1.1 Spatial pattern of phenological periodicity. Figure 3 shows the phenological parameter and the spatial distributions of start of growing season (SOS), end of
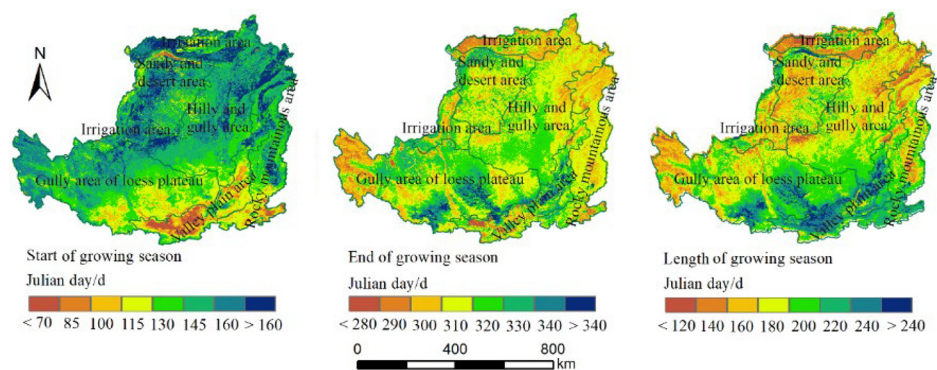
Figure 3.
Spatial patterns of phenological periodicity

Start of growing season
Julian day/d
< 70 85 100 115 130 145 160 > 160

End of growing season
Julian day/d
< 280 290 300 310 320 330 340 > 340
0   400   800
km

Length of growing season
Julian day/d
< 120 140 160 180 200 220 240 > 240

Source: Created by authors using ArcGIS (2019) solfware

growing season (EOS) and length of growing season (LOS). SOS was gradually later along the Southeast–Northwest direction, while EOS showed the opposite pattern. The vegetation started to grow earlier in the valley plain areas, which have relatively warm and humid climatic conditions. Vegetation started to grow latter in the northeast and northwest where climatic conditions are relatively dry and cold. The spatial variability of vegetation EOS was gradually postponed from north to south. LOS gradually shortened from southeast to northwest, while the southeast as a whole had longer LOS than the northwest. LOS in the southeast of the gully area of Loess Plateau and the valley plains area was longest.

3.1.2 Interannual variability of the phenological phase. The phenology variability of the Loess Plateau was fitted using linear regression to obtain trends for SOS, EOS and LOS (Figure 4). SOS, EOS and LOS showed significant changes in the southeast and northwest regions of the study area, while changes in the central region were relatively small showing a high - low - high trend along the Southeast–Northwest direction. LOS decreased in the valley plain areas and arid areas in the northwest, but gradually increased in the Fenhe River Basin and the western mountainous areas with higher elevations.

3.2 Multi-dimensional changes of enhanced vegetation index during the growing season
3.2.1 Spatiotemporal changes of vegetation enhanced vegetation index. The spatial distributions of EVI values during SOS, EOS and LOS were obtained using raster statistics (Figure 5). EVI values were higher in the southeast and lower in the northwest, showing a gradual decrease from southeast to northwest. The highest value of LOS EVI were mainly distributed in the southeast of the gully area of the Loess Plateau, the valley plains areas and the rocky mountainous areas in the south and east of the study area, especially in the southeast of the gully area of the Loess Plateau. In addition, the irrigated area also showed a small distribution. Regions where SOS EVI < 0.2 accounted for 59.13% of the total area, regions with $0.2 \leq$ EVI < 0.3 accounted for 22.27% and regions with EVI ≥ 0.3 accounted for 18.60%. Regions with EOS EVI < 0.2 accounted for 78.95%, regions with $0.2 \leq$ EVI < 0.3 accounted for 20.36% and regions with EVI ≥ 0.3 accounted for 0.69%. In addition, 29.67% of
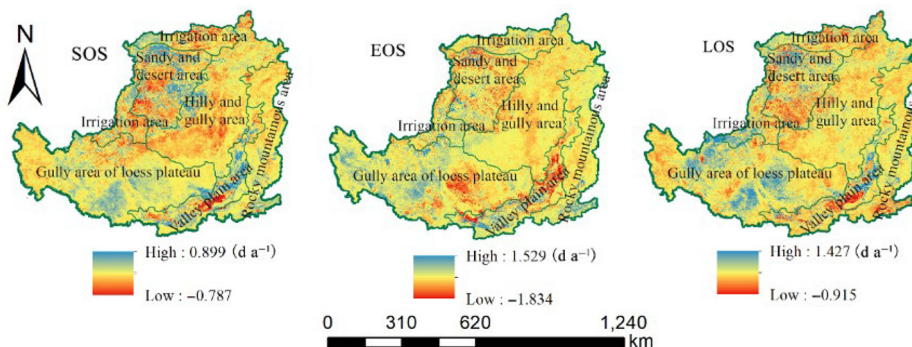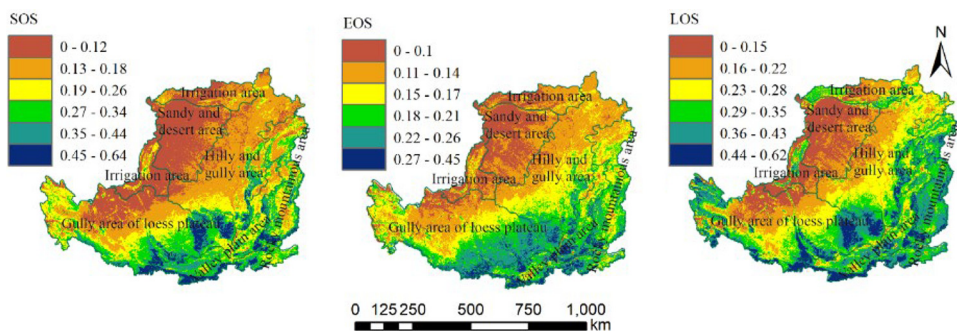

Figure 4.
Phenological change trend for the start of the growing season, length of the growing season, and end of the growing season

Source: Created by authors using ArcGIS (2019) solfware

Source: Created by authors using ArcGIS (2019) solfware

regions had LOS EVI < 0.2, 31.74% of regions had $0.2 \leq$ EVI < 0.3 and 38.59% of regions had EVI $\geq$ 0.3.

3.2.2 Vegetation enhanced vegetation index changes with different topographic factors. Along with a change in altitude, hydrothermal conditions also change and affect vegetation EVI. Analyzing EVI trends at different altitudes provides a deeper understanding of the changes in vegetation in the vertical direction. According to the percentage distribution of EVI at different elevations (Figure 6a), vegetation EVI values of SOS, EOS and LOS showed a high-low-high "valley type" distribution with increasing altitude. The SOS EVI percentage at minimum and maximum elevations was highest (15%). With increasing elevation, the percentage of EOS EVI changed from 16% to 14%, then decreased rapidly (11%), increased slightly and gradually leveled off (12%), thus showing strong zonality in the vertical direction.

The EVI percentage distributions at different slopes are shown in Figure 6 b: SOS EVI steadily increased from 7% to 15% with increasing slope. EOS EVI increased slowly with the increasing slope. LOS EVI increased rapidly and gradually stabilized. In summary, the percentages of SOS, EOS and LOS EVI gradually increased with increasing slope, but the rate of increase was different at different levels.

3.3 Response of vegetation to climate change

3.3.1 Temporal variability of the partial correlation between enhanced vegetation index and climatic factors. To explore the relationship between EVI, temperature and precipitation, partial correlations were calculated, alternatively using precipitation and temperature as control variables (Table 1). The partial correlation coefficients differed significantly. On a monthly scale, temperature exerted a stronger influence on EVI than precipitation. The maximum positive correlation between EVI and precipitation occurred in April (R = 0.90) and the minimum occurred in December (R = 0.79). The minimum negative correlation occurred in January and April (R = −0.80) and the maximum occurred in October (R = −0.90). Average values from April to July were positive. The maximum positive correlation between EVI and temperature occurred in February (R = 0.97) and the minimum occurred in December (R = 0.80). The minimum negative correlation occurred in December (R = −0.81) and the maximum occurred in February (R = −0.96).
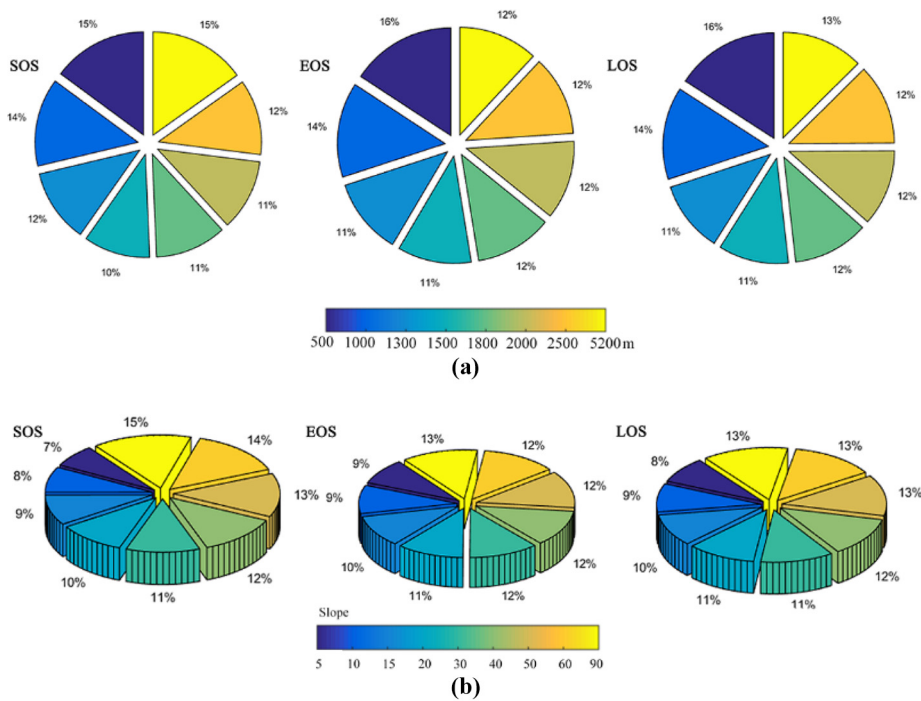
(a)

(b)

Source: Created by authors using MATLAB (2019) solfware

R-value	Jan	Feb	Mar	Apr	May	Jun	Jul	Aug	Sept	Oct	Nov	Dec
EVI-PRE												
(CV: TEM)												
Min	−0.80	−0.85	−0.84	−0.8	−0.86	−0.81	−0.83	−0.86	−0.87	−0.90	−0.84	−0.86
Max	0.81	0.89	0.84	0.9	0.87	0.85	0.88	0.82	0.85	0.84	0.84	0.79
Mean	−0.07	−0.02	−0.17	0.07	0.02	0.04	0.04	−0.09	−0.10	−0.16	0.00	−0.08
EVI-TEM												
(CV: PRE)												
Min	−0.92	−0.96	−0.91	−0.94	−0.95	−0.90	−0.91	−0.83	−0.92	−0.88	−0.88	−0.81
Max	0.87	0.97	0.91	0.90	0.92	0.92	0.85	0.88	0.92	0.93	0.90	0.80
Mean	−0.39	−0.48	−0.37	−0.40	−0.39	−0.35	−0.14	0.15	0.24	0.33	0.29	−0.05

Figure 6.
EVI percentages of
SOS, EOS, and LOS
at different elevations
(a) and slope
gradients (b)

Table 1.
Partial correlations
between EVI,
monthly
precipitation and
temperature

The average partial correlation coefficient between August and November was
positive, while it was negative in the remaining months.

*3.3.2 Spatial variability of partial correlations between enhanced vegetation index
and climatic factors.* To visualize the spatial variability of these results, partial correlation
coefficients were first calculated for EVI and precipitation while controlling for temperature.

Next, coefficients between EVI and temperature were calculated while controlling for precipitation (Figure 7).

After removing the influence of temperature, partial correlation coefficients between precipitation and EVI ranged between -0.849 and 0.907. After removing the influence of precipitation, partial correlation coefficients between temperature and EVI ranged between -0.911 and 0.852. Positive correlations between EVI and precipitation and negative correlations between EVI and temperature were mainly concentrated in the northwest of the gully area of the Loess Plateau and south of the hilly and gully area. Regions with significant negative correlations between EVI and precipitation and significant positive correlations between EVI and temperature were mainly concentrated in the southeastern gully area, southwest of the valley plains area and southeast of the rocky mountainous area.

4. Discussion

Empirical studies in China showed that vegetation activity was mainly regulated by temperature, which is especially pronounced in the mountainous regions of northern China. The vegetation EVI changes and responses to temperature and precipitation showed clear spatial differences and regularity. Temperature exerted a stronger influence on EVI than precipitation, which is consistent with the findings of relevant studies (Zhang et al., 2019; Qu et al., 2020). Ouyang et al. (2020) also reported that temperature exerted a stronger effect on vegetation of grassland and forest than precipitation in other basins by analyzing the correlation of vegetation with climatic factors.

With continuous global warming, empirical studies showed that the trend of the advancement of the phenological period is widespread. A similar phenomenon has been observed in this study, where the vegetation phenological clearly advanced over the past decade. This is relatively consistent with the results reported by other relevant literature (Hou et al., 2013), indicating that the extracted parameters based on reconstructed MODIS-EVI were reliable. Wang et al. (2019) used the relative threshold method to obtain the phenological parameters and also found a similar change, where the SOS and EOS showed earlier and later trends, respectively, which led to a longer LOS in the Yellow River Basin. The phenomenon of an elongated vegetation growth
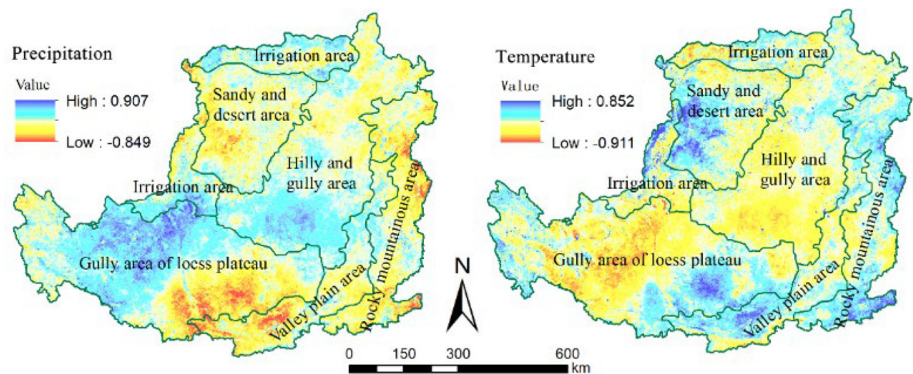

Figure 7.
Partial correlation
coefficients between
EVI, precipitation
and temperature

Source: Created by authors using ENVI/IDL (2019) solfware

season under the background of global warming has also been confirmed for other areas (Deng *et al.*, 2017). Furthermore, previous research showed that 54.84% of the area of the LOS was advanced, while 67.64% showed a delay in EOS and 66.28% had a lengthened LOS in the Loess Plateau (Wang *et al.*, 2016b).

This study adopted the S-G filtering algorithm, integrated in TIMESAT to reconstruct the time series MODIS EVI data and to remove noise, mutation points and noise from the original data set to ensure reliability of EVI data. In addition, the temperature and precipitation values were based on the interpolation of meteorological station data with the thin plate spline method. Although DEM were used for the interpolation, because of the scarcity of meteorological stations in mountainous areas, interpolation accuracy still remains uncertain. Therefore, selecting suitable satellite data based on the principle of availability and reliability is a feasible path worth exploring.

5. Conclusion

The phenological period of the Loess Plateau showed clear spatiotemporal heterogeneity. In terms of spatial variability, the SOS date of vegetation showed a gradually delaying trend from south to north. LOS gradually shorter from southeast to northwest. In terms of temporal variability, clear trends of an SOS advance and an EOS delay were found. Vegetation EVI change showed significant vertical zonality and gradually decreased from the southeast to the northwest under the influence of hydrothermal conditions. Partial correlation coefficients between vegetation EVI, temperature and precipitation indicated that temperature exerted a stronger impact on EVI than precipitation. Negative correlations between EVI and precipitation and positive correlations between EVI and temperature were mainly concentrated in the southwest of the valley plain area, southeast of the gully area and in the rocky mountainous area. Positive correlations between EVI and precipitation and negative correlations between EVI and temperature were mainly concentrated south of the hilly and gully area and northwest of the gully area of the Loess Plateau.

This study analyzed the spatial characteristics of phenological changes, based on the phenological changes of vegetation in the Loess Plateau over the past 20 years, which were retrieved based on long-time series remote sensing data sets. Scientific guidance for the plantation of plant species on the Loess Plateau can effectively increase the scientificity of ecological restoration projects. In addition, this study proved that the S-G filtering algorithm can effectively remove anomalies and noise from remote sensing image data. This effectively improves the accuracy of remote sensing data and yields better performance for the application of vegetation phenological change monitoring. This conclusion can provide a scientific and reasonable method for the preprocessing of remote sensing data for similar research.

Informed by this research, the authors suggest that the future directions of the driving forces of vegetation and phenological phase changes should focus on the following aspects: Firstly, the response of EVI to climate change should be studied on a longer time scale by combining this data with Global Inventory Modeling and Mapping Studies NDVI3g or similar data sets. Besides, the advantages of satellite data need to be used to simulate climate change in a more detailed way by downscaling satellite remote sensing data (Chen *et al.*, 2014; Chen *et al.*,2019). Secondly, the Chinese government has initiated a series of environmental protection measures that have directly caused land cover changes in the Loess Plateau since 1999 (Zhao *et al.*, 2017). The quantification and elimination of its influence on EVI change is an important issue for future studies. Finally, along with changes

in the global climate system and strong human interference, whether the warming trend will long-term development in Loess Plateau and surface process will be how to respond? Thirdly, while the temporal and spatial characteristics of EVI and its relationships with temperature and precipitation during the growing season have been studied in detail, EVI is not only affected by temperature and precipitation, but also by factors such as surface temperature, precipitation, evapotranspiration, wind speed, solar radiation and human activities. Therefore, the influence of the above factors to the vegetation patterns and dynamics of ecologically fragile areas require more comprehensive and continuous observation.

References

Adole, T., Dash, J., Rodriguez-Galiano, V. and Atkinson, P.M. (2019), "Photoperiod controls vegetation phenology across Africa", *Communications Biology*, Vol. 2 No. 1, pp. 1-13.

ArcGIS (2019), available at: www.esri.com/zh-cn/arcgis/about-arcgis/overview

Baniya, B., Tang, Q., Pokhrel, Y. and Xu, X. (2019), "Vegetation dynamics and ecosystem service values changes at national and provincial scales in Nepal from 2000 to 2017", *Environmental Development*, Vol. 32, p. 100464.

Borges, E.F., Sano, E.E. and Medrado, E. (2014), "Radiometric quality and performance of TIMESAT for smoothing moderate resolution imaging spectroradiometer enhanced vegetation index time series from Western Bahia state", *Journal of Applied Remote Sensing*, Vol. 8 No. 1, p. 083580.

Chen, F.R., Liu, Y., Liu, Q. and Li, X. (2014), "Spatial downscaling of TRMM 3B43 precipitation considering spatial heterogeneity", *International Journal of Remote Sensing*, Vol. 35 No. 9, pp. 3074-3093.

Chen, F.R., Gao, Y.Q., Wang, Y.G., Qin, F. and Li, X. (2019), "Downscaling satellite-derived precipitaiton products with an integrated framework", *International Journal of Climatology*, Vol. 39 No. 3, pp. 1287-1304.

Cleophas, T.J. and Zwinderman, A.H. (2018), *Regression Analysis in Medical Research*, Cham: Springer International Publishing.

Deka, J., Kalita, S. and Khan, M.L. (2019), "Vegetation phenological characterization of alluvial plain Shorea robusta-dominated tropical moist deciduous forest of northeast India using MODIS NDVI time series data", *Journal of the Indian Society of Remote Sensing*, Vol. 47 No. 8, pp. 1287-1293.

Deng, C., Bai, H., Zhai, D., Gao, S., Huang, X., Meng, Q. and He, Y. (2017), "Variation in plant phenology in the Qinling mountains from 1964-2015 in the context of climate change", *Acta Ecologica Sinica*, Vol. 37 No. 23, pp. 7882-7893.

Duarte, L., Teodoro, A.C., António, T., Monteiro, C. and Hernani, G. (2018), "QPhenoMetrics: an open source software application to assess vegetation phenology metrics", *Computers and Electronics in Agriculture*, Vol. 148, pp. 82-94.

ENVI/IDL (2019), available at: www.enviidl.com/

He, B.Z., Ding, J.L., Li, H., Liu, B.H. and Chen, W.Q. (2018), "Spatiotemporal variation of vegetation phenology in Xinjiang from 2001 to 2016", *Acta Ecologica Sinica*, Vol. 38 No. 06, pp. 2139-2155.

Hou, X.H., Niu, Z., Gao, S. and Huang, N. (2013), "Monitoring vegetation phenology in farming-pastoral zone using SPOT-VGT NDVI data", *Transactions of the Chinese Society of Agricultural Engineering*, Vol. 29 No. 1, pp. 142-150.

Huang, Y. (2009), "Reconstruction of MODIS-EVI time-series data with S-G filter", *Geomatics and Information Science of Wuhan University*, Vol. 34 No. 12, pp. 1440-1443.

IPCC (2014), "Contribution of working group I to the fifth assessment report of the intergovernmental panel on climate change", Climate Change 2014, *Cambridge University Press, Cambridge and New York, NY*.

Jonsson, P. and Eklundh, L. (2004), "TIMESAT - A program for analyzing time-series of satellite sensor data", *Computers and Geosciences*, Vol. 30 No. 8, pp. 833-845.

Liu, X.F., Ren, Z.Y., Lin, Z.H., Liu, Y.X. and Zhang, D.H. (2013), "The spatial-temporal changes of vegetation coverage in the three-river headwater region in recent 12 years", *Acta Geographica Sinica*, Vol. 68 No. 7, pp. 897-908.

Li, S.S., Yan, J.P. and Wan, J. (2012), "The spatial-temporal changes of vegetation restoration on loess Plateau in Shaanxi-Gansu-Ningxia region", *Journal of Geographical Sciences*, Vol. 23 No. 1, pp. 98-108.

Li, Y., Xie, Z.X., Qin, F., Qin, Y.C., Zheng, Z.C., Xia, H.M. and Zhang, L.J. (2019), "Geomorphological characteristics of a transect from the yellow river to the iron pagoda in Kaifeng city", *Carpathian Journal of Earth and Environmental Sciences*, Vol. 14 No. 1, pp. 245-254.

Madden, H. (1978), "Comments on the Savitzky-Golay convolution method for least-squares fit smoothing and differentiation of digital data", *Analytical Chemistry*, Vol. 50 No. 9, pp. 1383-1386.

MATLAB (2019), available at: ww2.mathworks.cn/products/get-matlab.html?s_tid=gn_getml

Merrick, T., Pau, S., Jorge, M.L.S.P., Silva, T.S. and Bennartz, R. (2019), "Spatiotemporal patterns and phenology of tropical vegetation solar-induced chlorophyll fluorescence across Brazilian biomes using satellite observations", *Remote Sensing*, Vol. 11 No. 15, pp. 1746.

Moreira, A., Fontana, D.C., Kuplich, T.M. and Guasselli, L.A. (2019), "Phenological metrics of the grassland vegetation of Rio Grande Do Sul, Brazil", *Revista Brasileira de Engenharia Agrícola e Ambiental*, Vol. 23 No. 12, pp. 899-906.

Ouyang, W., Wan, X., Xu, Y., Wang, X. and Lin, C. (2020), "Vertical difference of climate change impacts on vegetation at temporal-spatial scales in the upper stream of the Mekong river basin", *Science of the Total Environment*, Vol. 701, p. 134782.

Qu, S., Wang, L., Lin, A., Yu, D. and Yuan, M. (2020), "Distinguishing the impacts of climate change and anthropogenic factors on vegetation dynamics in the Yangtze river Basin", *Ecological Indicators*, Vol. 108, p. 105724.

Richardson, A.D., Keenan, T.F., Migliavacca, M., Ryu, Y., Sonnentag, O. and Toomey, M. (2013), "Climate change, phenology, and phenological control of vegetation feedbacks to the climate system", *Agricultural and Forest Meteorology*, Vol. 169 No. 2, pp. 156-173.

Silveira, E.M.D.O., Espírito-Santo, F.D.B., Acerbi-Júnior, F.W., Galvão, L.S., Withey, K.D., Blackburn, G.A., Mello, J.M., Shimabukuro, Y.E., Domingues, T. and Scolforo, J.R.S. (2019), "Reducing the effects of vegetation phenology on change detection in tropical seasonal biomes", *GIScience and Remote Sensing*, Vol. 56 No. 5, pp. 699-717.

Song, N.P., Du, L.T. and Wang, L. (2015), "Vegetation dynamics over 2000-2012 and its driving factors in Yanchi county, Ningxia province", *Acta Ecologica Sinica*, Vol. 35 No. 22, pp. 7377-7386.

Sousa, D., Small, C., Spalton, A. and Kwarteng, A. (2019), "Coupled spatiotemporal characterization of monsoon cloud cover and vegetation phenology", *Remote Sensing*, Vol. 11 No. 10, p. 1203.

Stisen, S., Sandholt, I., Norgaard, A., Fensholt, R. and Eklundh, L. (2007), "Estimation of diurnal air temperature using MSG SEVIRI data in West Africa", *Remote Sensing of Environment*, Vol. 110 No. 2, pp. 262-274.

Thompson, J.A. and Koenig, L.S. (2018), "Vegetation phenology in Greenland and links to cryospheric change", *Annals of Glaciology*, Vol. 59 No. 77, pp. 59-68.

TIMESAT (2019), available at: http://web.nateko.lu.se/timesat/timesat.asp?cat=0

Wang, Y., Luo, Y. and Shafeeque, M. (2019), "Interpretation of vegetation phenology changes using daytime and night-time temperatures across the yellow river basin", *Science of the Total Environment*, Vol. 693, pp. 133553.

Wang, Q.X., Fan, X.H., Qin, Z.D. and Wang, M.B. (2012), "Change trends of temperature and precipitation in the loess Plateau region of China, 1961–2010", *Global and Planetary Change*, Vol. 92-93, pp. 138-147.

Wang, Y.H., Zhao, M.F., Kang, M.Y. and Zuo, W.Y. (2016a), "Spatial scale-dependent and non-stationarity relationships between NDVI and climatic factors in the loess Plateau", *Geographical Research*, Vol. 35 No. 3, pp. 493-503.

Wang, K.Q., Yu, X.F., Shu, Q.T., Shang, K. and Wen, K.G. (2015), "Comparison on three algorithms of reconstructing time-series MODIS EVI", *Journal of Geo-Information Science*, Vol. 17 No. 6, pp. 732-741. Vol No

Wang, H., Liu, G.H., Li, Z.S., Ye, X., Wang, M. and Gong, L. (2016b), "Driving force and changing trends of vegetation phenology in the loess Plateau of China from 2000 to 2010", *Journal of Mountain Science*, Vol. 13 No. 5, pp. 844-856.

Xia, H.M., Li, A.N., Zhao, W., Bian, J.H. and Lei, G.B. (2015), "Spatiotemporal variations of Forest phenology in the Qinling zone based on remote sensing monitoring", *Progress in Geography*, Vol. 34 No. 10, pp. 1297-1305, 2001-2010.

Xia, H.M., Li, A.N., Feng, G., Li, Y., Qin, Y.C., Lei, G.B. and Cui, Y.P. (2018), "The effects of asymmetric diurnal warming on vegetation growth of the Tibetan Plateau over the past three decades", *Sustainability*, Vol. 10 No. 4, p. 1103.

Xin, Q.C., Broich, M., Zhu, P. and Gong, P. (2015), "Modeling grassland spring onset across the Western United States using climate variables and MODIS-derived phenology metrics", *Remote Sensing of Environment*, Vol. 161 No. 5, pp. 63-77.

Xu, Q.Y., Yang, G.J., Long, H.L., Wang, C.C., Li, X.C. and Huang, D.C. (2014), "Crop information identification based on MODIS NDVI time-series data", *Transactions of the Chinese Society of Agricultural Engineering*, Vol. 30 No. 11, pp. 134-144.

Yang, Z.Q., Dong, J.W., Xu, X.L., Zhao, G.S., Chen, W. and Zhou, Y. (2018), "Spatiotemporal pattern of Forest fragmentation in the loess Plateau", *Resources Science*, Vol. 40 No. 6, pp. 1246-1255.

Zhang, H. and Ren, Z.Y. (2015), "Remote sensing analysis of vegetation phenology characteristics in Shaanxi province based on Whittaker smoother method", *Journal of Desert Research*, Vol. 35 No. 4, pp. 1-6.

Zhang, C., Ren, Z.Y. and Wei, Z.F. (2013), "Vegetation responses to intra annual hydrothermal conditions on the loess Plateau", *Resources Science*, Vol. 35 No. 10, pp. 2017-2023.

Zhang, X.D., Zhu, W.B., Zhang, J.J., Zhu, L.Q., Zhao, F. and Cui, Y.P. (2018), "Phenology of forest vegetation and its response to climate change in the Funiu mountains", *Acta Geographica Sinica*, Vol. 73 No. 1, pp. 41-53.

Zhang, Y., Xu, G., Li, P., Li, Z., Wang, Y., Wang, B., Jia, L., Cheng, Y., Zhang, J., Zhuang, S. and Chen, Y. (2019), "Vegetation change and its relationship with climate factors and elevation on the Tibetan Plateau", *International Journal of Environmental Research and Public Health*, Vol. 16 No. 23, p. 4709.

Zhao, Z.Q., Gao, J.B., Wang, Y.L., Liu, J.G. and Li, S.C. (2014), "Exploring spatially variable relationships between NDVI and climatic factors in a transition zone using geographically weighted regression", *Theoretical and Applied Climatology*, Vol. 120 Nos 3/4, pp. 507-519.

Zhao, A.Z., Zhang, A.B., Liu, H.X., Liu, Y.X., Wang, H.F. and Wang, D.L. (2017), "Spatiotemporal variation of vegetation coverage before and after implementation of grain for Green project in the loess Plateau", *Journal of Natural Resources*, Vol. 32 No. 3, pp. 449-460.

Zhou, J.H., Cai, W.T., Qin, Y., Lai, L.M., Guan, T.Y., Zhang, X.L., Jiang, L.H., Du, H., Yang, D.W., Cong, Z.T. and Zheng, Y.R. (2016), "Alpine vegetation phenology dynamic over 16 years and its covariation with climate in a semi-arid region of China", *Science of the Total Environment*, Vol. 572, pp. 119-128.

Corresponding author
Yaochen Qin can be contacted at: qinyc@henu.edu.cn